

## Supplemental Information

### A pH-Regulated Quality Control Cycle for Surveillance of Secretory Protein Assembly

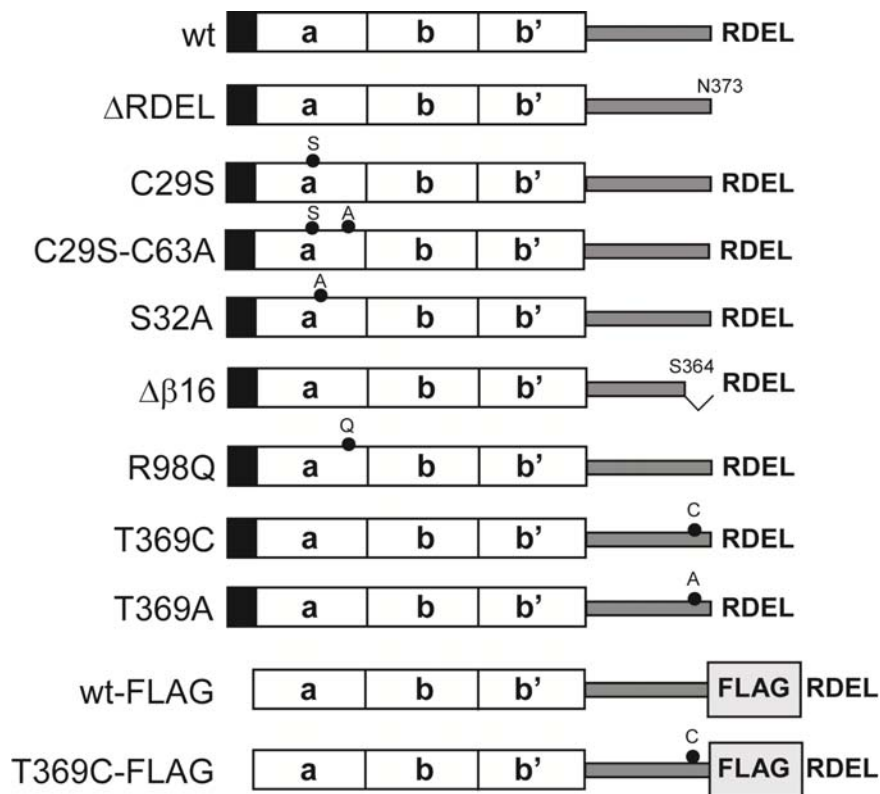
Stefano Vavassori, Margherita Cortini, Shoji Masui, Sara Sannino, Tiziana Anelli, Imma R. Caserta, Claudio Fagioli, Maria F. Mossuto, Arianna Fornili, Eelco van Anken, Massimo Degano, Kenji Inaba, and Roberto Sitia

#### *Inventory of Supplemental Information*

Supplemental Information provides 3 Supplemental Figures, 1 Supplemental Table, Supplemental Experimental Procedures, and Supplemental References; a brief description is given below.

- Supplemental Figure 1 (S1) provides a schematic representation of all ERp44 mutants used throughout the study.
- Supplemental Figure 2 (S2) shows a schematic representation of the transfection protocol used for the *in vivo* studies and an extended version of Figure 3B.
- Supplemental Figure 3 (S3) provides *in vivo* analysis of pH sensor mutants related to Figure 5. Non reducing gels for ERp44 mutants are shown in panel A while a comparative analysis of adiponectin secretion in the presence of the indicated mutants is shown in panel B.
- Supplemental Table 1 (S1) shows a list of all the primers employed throughout the study to generate ERp44 mutants.
- Supplemental Experimental Procedures provide details on the molecular dynamics simulation described in the main text in the paragraph entitled “*pH-regulation of C-tail opening accounts for ERp44 activity and involves protonation of the active site C29*”.
- Supplemental References are related to the Supplementary Experimental Procedures.

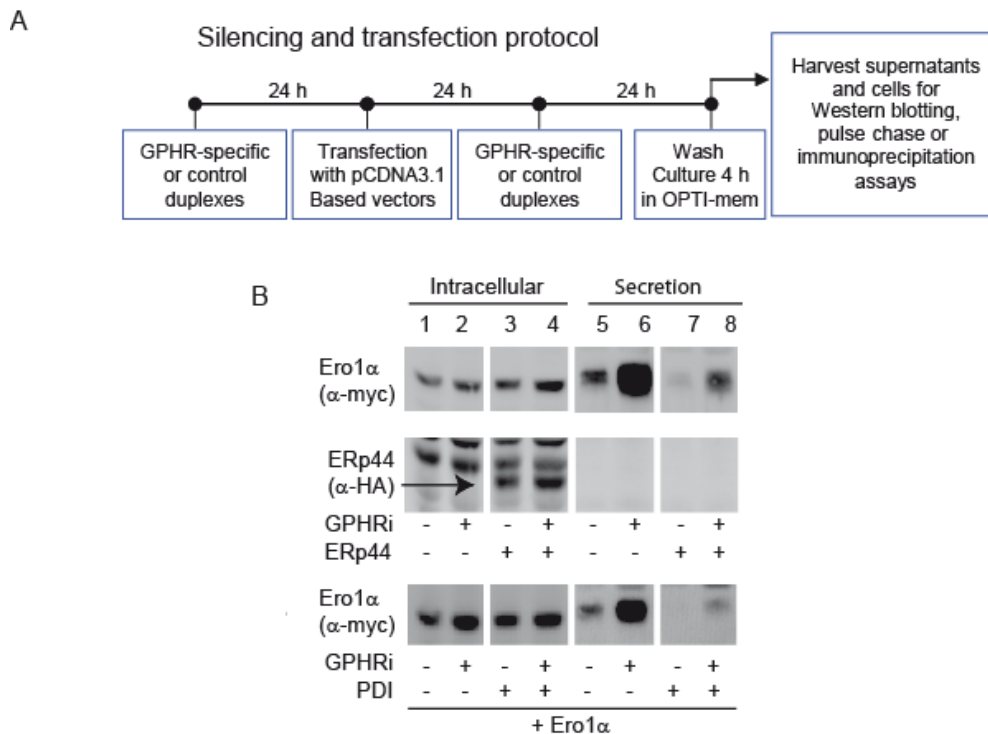
**Supplemental Figures and Legends**



*Supplemental Figure 1 (S1): Schematic representation of ERp44 mutants used in this study and related to all main text figures.*

The three thioredoxin-like domains **a**, **b**, and **b'** are depicted as white rectangles. The C-tail is shown in grey. The FLAG is boxed in light grey. The C-terminal RDEL retention motif is indicated. The black square at N-terminus represents the HA tag, placed immediately downstream of the signal sequence. All constructs expressed in *E. coli* that were used in *in vitro* studies lack the tag, the N-terminal hydrophobic signal sequence and the C-terminal – RDEL motif. The latter is not resolved in the published crystal structure (PDB code: 2R2J, Wang et al., 2008) suggesting its high flexibility.

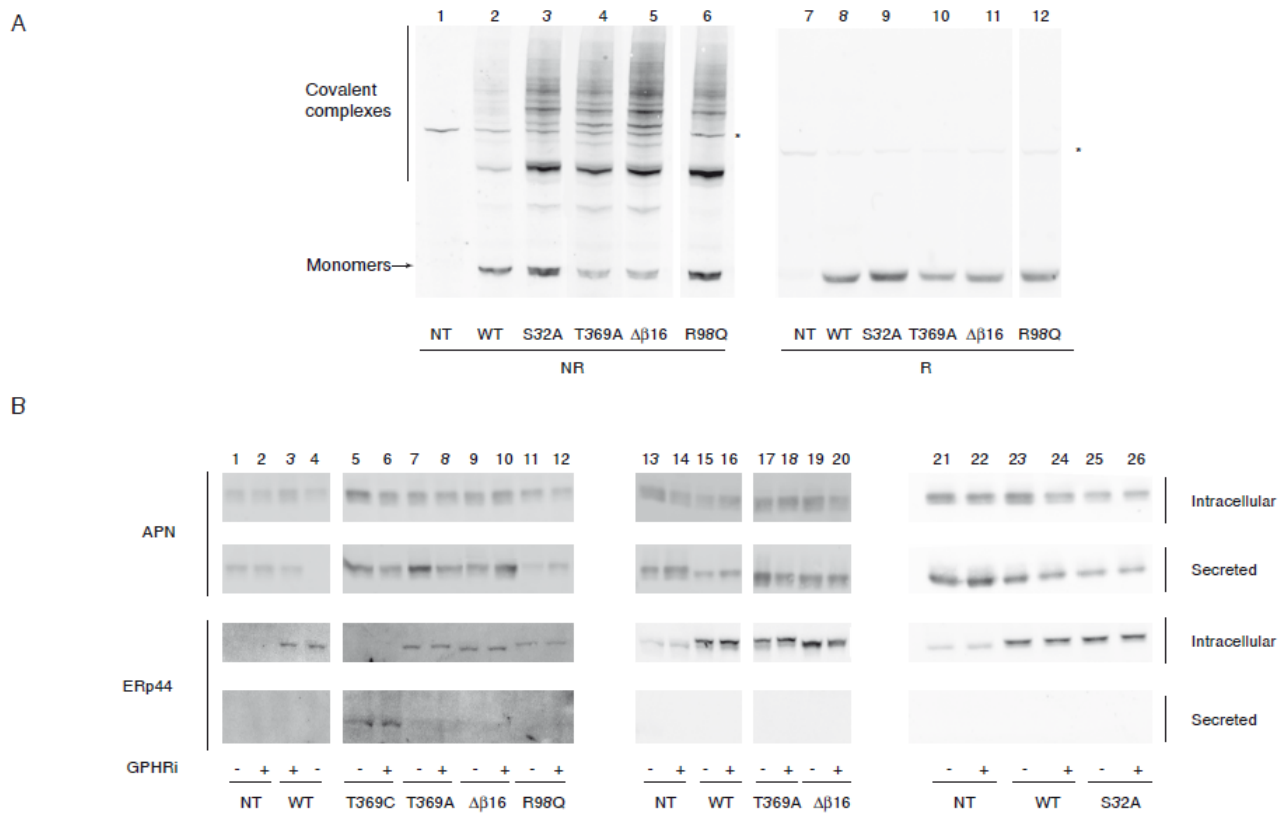
Black circles denote residues that were modified to the indicated residues by site directed mutagenesis. The coding sequence was severed at the indicated residues in deletion mutants (not in scale).



Supplemental Figure 2 (S2): The pH gradient along the early secretory compartment specifically regulates ERp44-mediated protein quality control (see also Figure 3).

A) Scheme of the transfection and silencing experiments shown in panel B and Fig. 3B-E. HeLa cells were silenced with specific or control oligonucleotides 72 and 24 h before analysis. Transfections were performed 48 h before analysis. Efficiency of GPHR silencing routinely exceeded 75%, as determined by mRNA quantification (not shown).

B) ERp44- but not PDI-mediated Ero1 $\alpha$  retention is pH sensitive. HeLa transfectants expressing Ero1 $\alpha$  alone or in conjunction with ERp44 or PDI were silenced with GPHR-specific or irrelevant siRNA. Lysates (Intracellular) and culture media (Secretion) were analyzed as in Fig. 3. The arrow points at over-expressed HA-tagged ERp44. Upper right panels for Ero1 $\alpha$  secretion are identical to those in Fig. 3B. The slight increase in Ero1 $\alpha$  secretion in PDI overexpressing cells (lane 8 of lower panel in part B of the Figure) likely reflects a residual role of ERp44 in Ero1 $\alpha$  retention (Otsu et al., 2006).



*Supplemental Figure 3 (S3), related to figure 5: In vivo analysis of pH sensor mutants.*

A) Aliquots of HeLa transfectants expressing the indicated mutants were resolved under non reducing (NR) and reducing (R) conditions and decorated with anti HA antibody. Arrows indicate over-expressed monomeric ERp44. The \* denotes a background band cross-reacting with our antibodies.

B) HeLa transfectants expressing the indicated ERp44 mutants and adiponectin under GPHRi or control conditions were washed and cultured for 4 hours in fresh medium (see Fig. S2). Aliquots of the lysates (Intracellular) and culture media (Secretion) were resolved under reducing conditions and decorated with anti-adiponectin (APN), anti-HA or anti-ERp44 (36C9) antibodies, as indicated. Representative experiments are shown for different ERp44 mutants (S32A, R98Q, T369A, T369C,  $\Delta\beta16$ ).

### ***Supplemental Experimental Procedures and Supplemental References***

#### *Molecular dynamics simulations*

The X-ray structure of ERp44 (PDB code 2R2J) was used to prepare the starting configuration for molecular dynamics (MD) simulations. The  $\Delta\beta 16$  structure was generated by deleting the coordinates of the Glu365-Arg372 segment. The missing loop in the **a** domain (Phe50-Glu53) was modelled with the ModLoop server (Fiser et al., 2000). The resulting structure was immersed in a cubic box ( $\sim 97 \times 97 \times 97 \text{ \AA}^3$ ) of  $\sim 29,000$  TIP3P water molecules and 13  $\text{Na}^+$  counterions. Simulations and subsequent analyses were performed with GROMACS 3.3.3., using the ff-amber99sb porting (Sorin and Pande, 2005) of the AMBER parm99SB parameter set (Hornak et al., 2006). Periodic boundary conditions were imposed. The equations of motion were integrated using the leap-frog method with a 1-fs time step. The Berendsen algorithm was employed for temperature ( $T=300 \text{ K}$ ) and pressure ( $p=1 \text{ bar}$ ) regulation, with coupling constants of 0.1 ps. Bonds to hydrogen atoms were frozen with the LINCS method for the protein and the ligand, while SETTLE was used for water molecules. The Particle Mesh Method was used to calculate electrostatic interactions, with a 11- $\text{\AA}$  cutoff for the direct space sums, a 1.0- $\text{\AA}$  FFT grid spacing and a 6-order interpolation polynomial for the reciprocal space sums. For van der Waals interactions, a switching function was used with a double 9-10  $\text{\AA}$  cut-off. Long-range corrections to the dispersion energy were also included (Shirts et al., 2007). The system was first minimized with 2000 steps of steepest descent. Harmonic positional restraints (with a force constant of  $\sim 12 \text{ kcal/mol/ \AA}^2$ ) were then imposed onto the protein heavy atoms and gradually turned off in 400 ps, while the temperature was increased from 200 to 300 K. The system was then simulated for 5 ns. To assess the reproducibility of the results, two trajectories were generated

for the wild type protein following the same protocol. The  $\Delta\beta 16$  protein simulation was prolonged to 10 ns.

	Primers	Template	Plasmid		ERp44
Fw	GCACCCAGTGAATATAGGTATTGTCTATTGAGGGATTAACCTCG	pET28 ERp44 wt	PET28	SDM	ERp44 T369C
Rv	CGAGTTAATCCCTCAATAGACAATACCTATATTTCACTGGGTGC				
Fw	GTAATTTTATGCTGACTGGGCTCGTTTCAGTCAGATGTTGC	pET28 ERp44 wt	PET28	SDM	ERp44C29A
Rv	GCAACATCTGACTGAAACGAGCCAGTCAGCATAAAAAATTAC				
Fw	CACCCAGTGAATATAGGTATTGTCTATTGAGGGATCGAGATG	pCDNA ERp44 wt	pcDNA	SDM	ERp44T369C
Rv	CATCTCGATCCCTCAATAGACAATACCTATATTTCACTGGGTG				
Fw	CCCAGCGAGTATAGGTATTGTTTATTGAGGGATCGAG	pEGFP N1	pEGFP N1	SDM	ERp44T369C Flag
Rv	CTCGATCCCTCAATAACAATACCTATACTCGTGGG	ERp44-Flag			
Fw	GTAATTTTATGCTGACTGGGCTCGTTTCAGTCAGATGTTGC	pCDNA ERp44 wt	pcDNA	SDM	ERp44C29A
Rv	GCAACATCTGACTGAAACGAGCCAGTCAGCATAAAAAATTAC				
Fw	CCTCCAGAACTAGCACCCAGTTAATATAGGTATACTTATTGAGG	pCDNA ERp44 wt	pcDNA	SDM	ERp44Δβ16
Rv	CCTCAATAGAGTATACTATATTAAGTGGGTGCTAGTTTCTGGAAGG				
Fw	CAACTCGAGCGTTACCATGCATCCTGCC	pCDNA ERp44 wt	pcDNA	PCR	ERp44Δβ16
Rv	GCGCGGTACCTTAAAGCTCATCTCGACTGGGTGCTAGTTTCTGGAAG			cloning	
Fw	GAGAATACAGGGTCCAGCAGTCAGTCAAAGCATTGGC	pET28 ERp44 wt	PET28	SDM	ERp44R98Q
Rv	GCCAAATGCTTTCACTGACTGCTGACCCCTGTATTCTC				
Fw	GAGAATACAGGGTCCAGCAGTCAGTCAAAGCATTGGC	pCDNA ERp44 wt	pcDNA	SDM	ERp44R98Q
Rv	GCCAAATGCTTTCACTGACTGCTGACCCCTGTATTCTC				
Fw	GAAACTAGCACCCAGTGAATATCAGTATACTTATTGAGGGATCG	pCDNA ERp44 wt	pcDNA	SDM	ERp44R367Q
Rv	CGATCCCTCAATAGAGTATACTGATATTCACTGGGTGCTAGTTTC				
Fw	GCACCCAGTGAATATCAGTATACTTATTGAGG	pET28 ERp44 wt	PET28	SDM	ERp44R367Q
Rv	CCTCAATAGAGTATACTGATATTCACTGGGTGCTG				
Fw	TTTGCCAGAGTTGATGCGGATCAGCACTCTGAC	pET28 ERp44	PET28	SDM	ERp44C29A
Rv	GTCAGAGTGCTGATCGGCATCAACTCTGGCAAA	C29A			C63A
Fw	GCTGACTGGTTCGTTTCGCTCAGATGTTGCATCCAATT	pCDNA ERp44 wt	pcDNA	SDM	ERp44S32A
Rv	AATTGGATGCAACATCTGAGCGAAACGACACCCAGTCAGC				

*Supplemental Table S1:* List of the primers and methods (SDM, side directed mutagenesis; PCR, polymerase chain reaction) employed to generate ERp44 mutants used in all main text figures.

### ***Supplemental References***

Fiser, A., Do, R.K., and Sali, A. (2000). Modeling of loops in protein structures. *Protein Sci* 9, 1753-1773.

Hornak, V., Abel, R., Okur, A., Strockbine, B., Roitberg, A., and Simmerling, C. (2006). Comparison of multiple Amber force fields and development of improved protein backbone parameters. *Proteins* 65, 712-725.

Shirts, M.R., Mobley, D.L., Chodera, J.D., and Pande, V.S. (2007). Accurate and efficient corrections for missing dispersion interactions in molecular simulations. *J Phys Chem B* 111, 13052-13063.

Sorin, E.J., and Pande, V.S. (2005). Empirical force-field assessment: The interplay between backbone torsions and noncovalent term scaling. *J Comput Chem* 26, 682-690.